Automatic magnetic compensation system for SERF atomic comagnetometer

Zhuo Wang, Luxv Zhai, Jiong Huang
Research Institute for Frontier Science
Beihang University
Beijing, China
zhuowang@buaa.edu.cn, 940072929@qq.com, huangjiong@buaa.edu.cn

2020 35th Youth Academic Annual Conference of Chinese Association of Automation (YAC) | 978-1-7281-7684-0/20/$31.00 ©2020 IEEE | DOI: 10.1109/YAC51587.2020.9337652

Abstract—To realize the SERF (spin exchange relaxation free) state of the atomic comagnetometer for inertial measurement, this paper proposes an efficient automatic magnetic compensation system based on the analysis of the dynamic model of the SERF atomic comagnetometer, such that the essential and necessary condition of low environmental magnetic field is satisfied. This system first makes a fast but rough compensation to reduce the impact of environmental magnetic field to a very low level, then accurately but slowly compensates the residual magnetic field. The rough compensation is made under low power detection light to achieve high efficiency, while the accurate one is made under high power detection light to achieve high accuracy, which are both automatically performed. This is definitely an advantage over the most existing magnetic compensation systems for the SERF atomic comagnetometer, which rely only on manual adjustments with low accuracy and poor repeatability. The simulation illustrates the good efficiency, accuracy and repeatability of the proposed automatic magnetic compensation system.

Keywords—SERF atomic comagnetometer; automatic magnetic compensation; high efficiency; high accuracy; repeatability

I. INTRODUCTION

Inertial navigation and guidance technology are widely used in aerospace and various fields of national economy. As the core component of this technology, comagnetometer has a direct impact on navigation precision. High-precision comagnetometers are urgently needed for long-range and long-endurance inertial navigation and guidance [1]. The SERF atomic comagnetometer has become a research hotspot because of its high precision and small size [2].

The key to the SERF atomic comagnetometer is to realize the SERF state. Laser pumping, high density particle and low magnetic field environment are the key to the realization of SERF state [3]. Among them, the low magnetic field environment is one of the important factors affecting the comagnetometer. The implementation of low magnetic field environment is mainly divided into passive magnetic shielding and active magnetic compensation. The passive magnetic shielding can only shield the environmental magnetic field on the order of 1nT, so it requires high precision active magnetic compensation technology to reduce the environmental magnetic field on the order of 1pT [4].

At present, the traditional magnetic compensation method is mainly through manual magnetic compensation, it not only has low efficiency, but also has low precision. In this paper, active magnetic compensation is divided into two parts based on the common characteristics of atomic comagnetometer and magnetometer. First, using the low-power laser pump the cell. At this time, the comagnetometer can be approximately regarded as a magnetometer, and in-situ triaxial magnetic field compensation method can be used to quickly make rough compensation. Then, increase the pumping power to hyperpolarize the nucleus, using cross modulation method for fine compensation.

The whole set of automatic magnetic compensation system uses self-made data acquisition board, and uses LabVIEW and FPGA (Field Programmable Gate Array) to achieve the program of automatic magnetic field compensation.

II. THE COMPOSITION OF AUTOMATIC MAGNETIC COMPENSATION SYSTEM

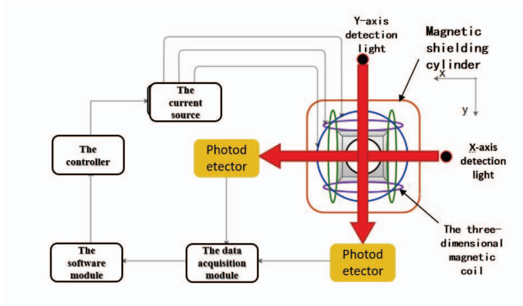

Fig. 1. *The composition of nuclear spin compensation system of the atomic comagnetometer.*

The block diagram of the nuclear spin magnetic field self-compensation system of the SERF atomic comagnetometer is shown in figure 1.

The detection optical route is comprised of detection laser, polarizer, analyzer and photodetector. The system uses biaxial detection technology, which is applied the detection laser in X and Y directions. The biaxial detection technology which measure date at the same time can improve system accuracy.

This research was supported by National Natural Science Foundation of China (Grant 61673041) and BAQIS Research Program: Y18G34.

Passive magnetic shielding can attenuate the geomagnetic field of 5×10^4nT to 100pT [5]. However, the remaining magnetic field of 100pT still affects the SERF state of atomic comagnetometer, so the three-dimensional active magnetic compensation coil which can generate a compensation magnetic field with identical magnitude but opposite direction with the remaining magnetic field is used to compensate the remaining magnetic field. The active magnetic compensation can offset and avoid the interference caused by the large external disturbance of the remaining magnetic field on the atomic comagnetometer.

Due to the need of miniaturization of the SERF atomic comagnetometer, the data acquisition module adopts the data acquisition circuit board made by the laboratory. Two high-precision acquisition circuits are used to acquire the X and Y direction optical signals respectively to realize the control quantity acquisition of the magnetic compensation system.

The software based on FPGA can obtain the final magnetic compensation data by modulating the system magnetic field and analyzing and processing the detection signal, and input its current into the three-dimensional magnetic coil through a high-precision current source to precisely compensate the environmental magnetic field.

III. The Basic Principle of Automatic Magnetic Compensation System

This paper presents an automatic magnetic compensation system, which is divided into two parts: "rough" compensation and "accurate" compensation.

The "rough" compensation means that under the pumping of a low-power pumping laser, the alkali metal atoms are polarized, while the inert gas nucleons have not been hyperpolarized. The comagnetometer can be roughly regarded as a magnetometer. At this point, the Bloch equations describing the alkali metal atoms are as follows [6]:

$$\begin{pmatrix} \dot{P}_x^e \\ \dot{P}_y^e \\ \dot{P}_z^e \end{pmatrix} = \gamma_e \cdot \begin{pmatrix} B_x \\ B_y \\ B_z \end{pmatrix} \times \begin{pmatrix} P_x^e \\ P_y^e \\ P_z^e \end{pmatrix} + \begin{pmatrix} 0 \\ 0 \\ R_p \end{pmatrix} - \begin{pmatrix} R_2 P_x^e \\ R_2 P_y^e \\ R_1 P_z^e \end{pmatrix} \tag{1}$$

where $\vec{P}$ is the polarization of the alkali metal atoms in the cell, γ_e is the electron gyromagnetic ratio of the alkali metal atom, $\vec{B}$ is the magnetic field, R_p is the optical pumping rate, R_1 is the longitudinal relaxation rate, and R_2 is the transverse relaxation rate. Solving Eq. (1) in the steady state, we have:

$$\begin{cases} P_{ex} = R_{op}\gamma_e \dfrac{B_y R_2 + B_x B_z \gamma_e}{(B_x^2+B_y^2)\gamma_e^2 R_2 + B_z^2\gamma_e^2 R_1 + R_2^2 R_1} \\ P_{ey} = R_{op}\gamma_e \dfrac{-B_x R_2 + B_y B_z \gamma_e}{(B_x^2+B_y^2)\gamma_e^2 R_2 + B_z^2\gamma_e^2 R_1 + R_2^2 R_1} \\ P_{ez} = R_{op} \dfrac{B_z^2\gamma_e^2 + R_2^2}{(B_x^2+B_y^2)\gamma_e^2 R_2 + B_z^2\gamma_e^2 R_1 + R_2^2 R_1} \end{cases} \tag{2}$$

The pumping light of the system is in the direction of Z axis, and the voltage signal which is converted by the photodetector is proportional to P_{ez}. Since P_{light} and P_{ez} are both positive in our case, we define a positive coefficient k where

$$V_{light} = kP_{ez} \tag{3}$$

Substitute Eq. (3) into Eq. (2) to obtain:

$$V_{\text{light}} = kR_{op} \frac{B_z^2\gamma_e^2 + R_2^2}{(B_x^2 + B_y^2)\gamma_e^2 R_2 + B_z^2\gamma_e^2 R_1 + R_2^2 R_1} \tag{4}$$

Partial derivatives of Eq. (4) with respect to B_x, B_y, B_z are obtained as follows:

$$\begin{cases} \dfrac{\partial V_{light}}{\partial B_x} = \dfrac{-2kR_{op}R_2\gamma_e^2(B_z^2\gamma_e^2+R_2^2)B_x}{[(B_x^2+B_y^2)\gamma_e^2 R_2 + B_z^2\gamma_e^2 R_1 + R_2^2 R_1]^2} = k_{Bx}\cdot B_x \\ \dfrac{\partial V_{light}}{\partial B_y} = \dfrac{-2kR_{op}R_2\gamma_e^2(B_z^2\gamma_e^2+R_2^2)B_y}{[(B_x^2+B_y^2)\gamma_e^2 R_2 + B_z^2\gamma_e^2 R_1 + R_2^2 R_1]^2} = k_{Bx}\cdot B_x \\ \dfrac{\partial V_{light}}{\partial B_z} = \dfrac{2kR_{op}R_2\gamma_e^2(B_z^2\gamma_e^2+R_2^2)B_z}{[(B_x^2+B_y^2)\gamma_e^2 R_2 + B_z^2\gamma_e^2 R_1 + R_2^2 R_1]^2} = k_{Bx}\cdot B_x \end{cases} \tag{5}$$

It can be seen from (5) that, at this time: $B_x = 0, B_y = 0, B_z = 0$, the V_{light} corresponding two maxima and a minima were respectively, which were used as the criterion to make "rough" compensation for the triaxial magnetic field.

After the "rough" compensation is completed, the pumping light power will be increased to make the nucleus hyperpolarized, and then "accurate" compensation will be made. At this point, the corresponding Bloch equation is [7]:

$$\frac{\partial \mathbf{P}^e}{\partial t} = \frac{\gamma^e}{Q(P^e)}\left(\mathbf{B} + \lambda M^n\mathbf{P}^n + \mathbf{L}\right)\times\mathbf{P}^e - \mathbf{\Omega}\times\mathbf{P}^e + \frac{(R_p\mathbf{s}^p + R_{se}^{en}\mathbf{P}^n + R_m\mathbf{s}^m - R_{tot}\mathbf{P}^e}{Q(P^e)} \tag{6}$$

$$\frac{\partial \mathbf{P}^n}{\partial t} = \gamma^n\left(\mathbf{B} + \lambda M^e\mathbf{P}^e\right)\times\mathbf{P}^n - \mathbf{\Omega}\times\mathbf{P}^n + R_{se}^{ne}\left(\mathbf{P}^e - \mathbf{P}^n\right) - R_{sd}^n\mathbf{P}^n \tag{7}$$

Where $\mathbf{P}^e$ is the polarization of electron spin of the alkali metal atom, $\mathbf{P}^n$ is the polarization of nuclear spin of the noble gas atom, γ^e is the electron gyromagnetic ratio, and γ^n is the nuclear gyromagnetic ratio. $\mathbf{B}$ is the external magnetic fields, $\lambda M^n\mathbf{P}^n$ is the magnetic fields generated by nuclear spin and sensed by electron spin, $\lambda M^e\mathbf{P}^e$ is the magnetic fields generated by electron spin and sensed by nuclear spin, and $\mathbf{L}$ is light shift. $Q(P^e)$ is slowdown factor which is related to the P^e. R_p is pumping rate generated by the pump beam and $\mathbf{s}^p$ gives the pumping direction. R_m is detecting rate generated by the pump beam and $\mathbf{s}^m$ gives the pumping direction. $\mathbf{s}^p$ and $\mathbf{s}^m$ are the degree of circular polarization of pump light and detection light. R_{se}^{en} is the spin exchange pumping rate by nuclear spin, while the R_{se}^{ne} is the spin exchange pumping rate by electron spin. R_{tot} is the total relaxation rate of electron spin. R_{sd}^{n} is the collision relaxation rate of the inert gas atom. $\mathbf{\Omega}$ is the rotation vector that we want to measure.

Solving Eq. (6) and Eq. (7) in steady state, the correlation between the X-axis polarizability and the magnetic field was obtained [8]:

$$P_x^e(B_x)=\frac{\gamma^e P_z^e R_{tot}^e}{(R_{tot}^e)^2+(\gamma^e)^2(L_z+\delta B_z-Q\Omega_z/\gamma^e)^2}\frac{B_x}{B_c}\left(\frac{\gamma^e(L_z+\delta B_z)}{R_{tot}^e}\delta B_z+\frac{P_z^n R_{se}^{en}}{P_z^e\gamma^e}\right) \tag{8}$$

$$P_x^e(B_y)=\frac{\gamma^e P_z^e R_{tot}^e}{(R_{tot}^e)^2+(\gamma^e)^2(L_z+\delta B_z-Q\Omega_z/\gamma^e)^2}\frac{B_y\delta B_z}{B_c} \tag{9}$$

The correlation between Y-axis polarizability and magnetic field is obtained as follows:

$$P_y^e(B_x)=-\frac{\gamma^e P_z^e R_{tot}^e}{(R_{tot}^e)^2+(\gamma^e)^2(L_z+\delta B_z-Q\Omega_z/\gamma^e)^2}\frac{B_x\delta B_z}{B_c} \tag{10}$$

$$P_y^e(B_y)=\frac{\gamma^e P_z^e R_{tot}^e}{(R_{tot}^e)^2+(\gamma^e)^2(L_z+\delta B_z-Q\Omega_z/\gamma^e)^2}\frac{B_y}{B_c}\left(\frac{\gamma^e(L_z+\delta B_z)}{R_{tot}^e}\delta B_z+\frac{P_z^n R_{se}^{en}}{P_z^e\gamma^e}\right) \tag{11}$$

The analytical Eq. (9) is used to calculate the partial derivative of B_y, and the results are as follows:

$$\frac{\partial P_x^e(B_y)}{\partial B_y}\approx\frac{\gamma^e P_z^e}{(R_{tot}^e)}\frac{\delta B_z}{B_c} \tag{12}$$

The analytical Eq. (9) is used to calculate the partial derivative of δB_z, and the results are as follows:

$$\frac{\partial P_x^e(B_y)}{\delta B_z}\approx\frac{\gamma^e P_z^e}{(R_{tot}^e)}\frac{B_y}{B_c} \tag{13}$$

The analytical Eq. (10) is used to calculate the partial derivative of δB_z, and the results are as follows:

$$\frac{\partial P_y^e(B_x)}{\delta B_z}\approx-\frac{\gamma^e P_z^e}{(R_{tot}^e)}\frac{B_x}{B_c} \tag{14}$$

Analyzing Eq. (12), when δB_z changes to zero, P_x^e reaches the maximum value. Analyzing Eq. (13), when B_y changes to zero, P_x^e reaches the maximum value. Analyzing Eq. (14), when B_x changes to zero, P_y^e reaches the minimum value. According to the above analysis, the residual magnetic field is compensated by the "accurate" compensation.

IV. SOFTWARE DESIGN OF ATOMIC COMAGNETOMETER AUTOMATIC MAGNETIC COMPENSATION SYSTEM

Based on the above principles, the software of atomic comagnetometer automatic magnetic compensation system is designed based on FPGA development board.

"Rough" compensation software flow chart:

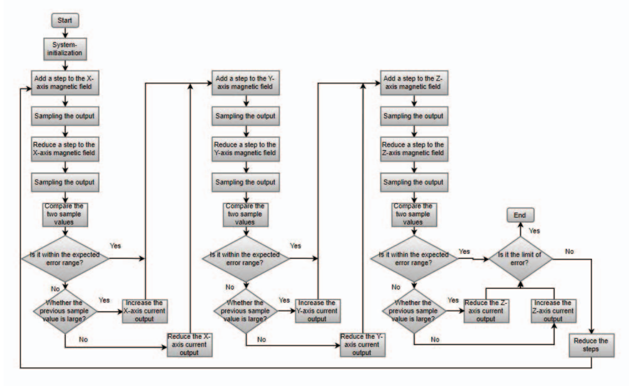

Fig. 2. *"Rough" compensation software flowchart.*

"Accurate" compensation software flow chart:

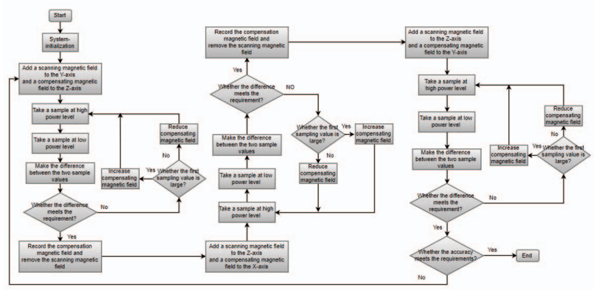

Fig. 3. *"Accurate" compensation software flowchart.*

V. SIMULATION ANALYSIS

The above two methods are simulated by Matlab software, and the results are as follows:

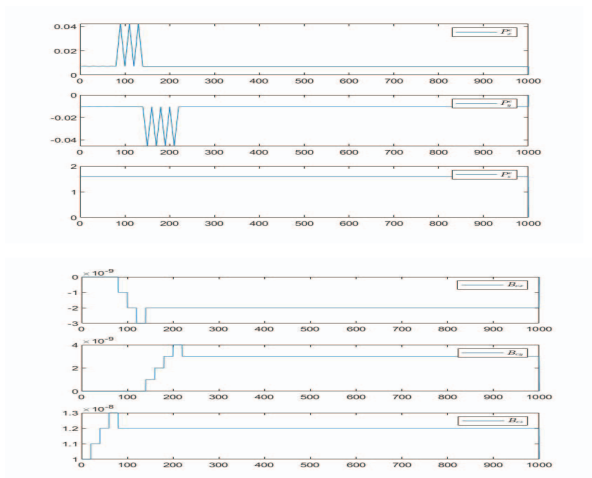

Fig. 4. *"Rough" compensation simulation.*

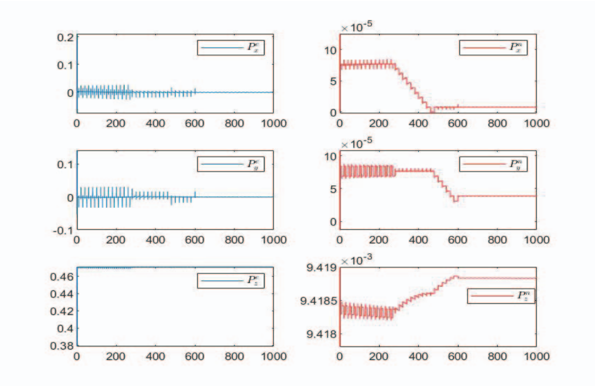

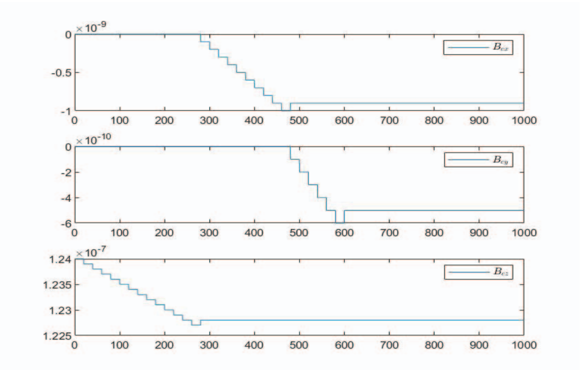

Fig. 5. *"Accurate" compensation simulation.*

According to the simulation results, the "rough" compensation can quickly compensate the environmental magnetic field to the level of 1nT. The "accurate" compensation can accurately compensate the environmental magnetic field to the level of 1pT. The atomic comagnetometer automatic magnetic compensation system can quickly and accurately compensate the environmental magnetic field, effectively suppress the interference of the external magnetic field, and enhance the SERF state of the atomic comagnetometer.

VI. THE CONCLUSION

Based on the study and modeling of the dynamics analysis of atomic spin comagnetometer, this paper presented an efficient, fast, accurate and highly repeatable automatic magnetic compensation system. This system based on FPGA program and integrated circuit board on the basis of simulation. The simulation results show that the system has a good effect. Next, the system needs to be put into the actual device for testing, and the experimental results should be observed and the system should be improved according to the experimental data.

ACKNOWLEDGMENT

The authors acknowledge Ruigang Wang (from Beihang University) for discussion and experiment assistance. This research was supported by National Natural Science Foundation of China (Grant 61673041) and BAQIS Research Program: Y18G34.

REFERENCES

[1] Fang J C , Qin J . Advances in Atomic Comagnetometers: A View from Inertial Navigation Applications[J]. SENSORS, 2012, 12(5):6331-6346.

[2] Seltzer S J , Romalis M V . Unshielded three-axis vector operation of a spin-exchange-relaxation-free atomic magnetometer[J]. Applied Physics Letters, 2004, 85(20):4804-4806.

[3] Savukov I., Romalis M. Effects of spin-exchange collisions in a high-density alkali-metal vapor in low magnetic fields[J]. Physical Review A, 2005, 71(2):023405

[4] Kuriki S., Hayashi A., Washio T., et al. Active compensation in combination withweak passive shielding for magnetocardiographic measurements[J]. Review ofScientificInstruments, 2002, 73(2): 440-445

[5] Budker D., Romalis M. Optical magnetometry[J]. Nature Physics, 2007, 3(4):227-234.

[6] Fang J , Qin J . In situ triaxial magnetic field compensation for the spin-exchange-relaxation-free atomic magnetometer[J]. Review of Scientific Instruments, 2012, 83(10):103104.

[7] Qin J , Fang J , Wan S . Experimental design of a dual axis Atomic Spin Comagnetometer[C]// Instrumentation and Control Technology (ISICT), 2012 8th IEEE International Symposium on. IEEE, 2012.

[8] Li Rujie, Quan Wei, Fan Wenfeng, Xing Li, Wang Zhuo, Zhai Yueyang, and Fang Jiancheng. A Dual-Axis, High-Sensitivity Atomic Magnetometer [J]. Chinese Physics B,